UNIVERSITY of York

This is a repository copy of *Inclusive cross sections for one- and multi-nucleon removal from Sn, Sb, and Te projectiles beyond the N = 82 shell closure*.

White Rose Research Online URL for this paper:
https://eprints.whiterose.ac.uk/id/eprint/163616/

Version: Published Version

Article:
Vaquero, V., Jungclaus, A., Rodríguez-Sánchez, J. L. et al. (31 more authors) (2019) Inclusive cross sections for one- and multi-nucleon removal from Sn, Sb, and Te projectiles beyond the N = 82 shell closure. Physics Letters, Section B: Nuclear, Elementary Particle and High-Energy Physics. pp. 356-361. ISSN: 0370-2693

https://doi.org/10.1016/j.physletb.2019.06.035

Reuse
This article is distributed under the terms of the Creative Commons Attribution (CC BY) licence. This licence allows you to distribute, remix, tweak, and build upon the work, even commercially, as long as you credit the authors for the original work. More information and the full terms of the licence here: https://creativecommons.org/licenses/

Takedown
If you consider content in White Rose Research Online to be in breach of UK law, please notify us by emailing eprints@whiterose.ac.uk including the URL of the record and the reason for the withdrawal request.

White Rose university consortium
Universities of Leeds, Sheffield & York

eprints@whiterose.ac.uk
https://eprints.whiterose.ac.uk/

Physics Letters B 795 (2019) 356–361

Contents lists available at ScienceDirect

Physics Letters B

www.elsevier.com/locate/physletb

Inclusive cross sections for one- and multi-nucleon removal from Sn, Sb, and Te projectiles beyond the $N = 82$ shell closure

V. Vaquero [a], A. Jungclaus [a,*], J.L. Rodríguez-Sánchez [b], J.A. Tostevin [c], P. Doornenbal [d], K. Wimmer [e,d], S. Chen [d,f], E. Nácher [a], E. Sahin [g], Y. Shiga [h], D. Steppenbeck [d], R. Taniuchi [d,e], Z.Y. Xu [i], T. Ando [e], H. Baba [d], F.L. Bello Garrote [g], S. Franchoo [j], A. Gargano [k], K. Hadynska-Klek [g], A. Kusoglu [l,m], J. Liu [i], T. Lokotko [i], S. Momiyama [e], T. Motobayashi [d], S. Nagamine [e], N. Nakatsuka [n], M. Niikura [e], R. Orlandi [o], T. Saito [e], H. Sakurai [d,e], P.A. Söderström [d], G.M. Tveten [g], Zs. Vajta [p], M. Yalcinkaya [l]

[a] Instituto de Estructura de la Materia, CSIC, E-28006 Madrid, Spain
[b] Universidad de Santiago de Compostela, E-15782 Santiago de Compostela, Spain
[c] Department of Physics, University of Surrey, Guildford, Surrey GU2 7XH, United Kingdom
[d] RIKEN Nishina Center, 2-1 Hirosawa, Wako, Saitama 351-0198, Japan
[e] Department of Physics, University of Tokyo, 7-3-1 Hongo, Bunkyo, Tokyo 113-0033, Japan
[f] School of Physics and State Key Laboratory of Nuclear Physics and Technology, Peking University, Bejing 100871, People's Republic of China
[g] Department of Physics, University of Oslo, NO-0316 Oslo, Norway
[h] Department of Physics, Rikkyo University, Tokyo, Japan
[i] Department of Physics, The University of Hong Kong, Pokfulam, Hong Kong
[j] Institut de Physique Nucléaire Orsay, IN2P3-CNRS, 91406 Orsay Cedex, France
[k] Istituto Nazionale di Fisica Nucleare, Complesso Universitario di Monte S. Angelo, I-80126 Napoli, Italy
[l] Department of Physics, Faculty of Science, Istanbul University, Vezneciler/Fatih, 34134, Istanbul, Turkey
[m] ELI-NP, Horia Hulubei National Institute of Physics and Nuclear Engineering, 077125 Magurele, Romania
[n] Department of Physics, Faculty of Science, Kyoto University, Kyoto 606-8502, Japan
[o] Advanced Science Research Center, Japan Atomic Energy Agency, Tokai, Ibaraki 319-1195, Japan
[p] MTA Atomki, P.O. Box 51, Debrecen H-4001, Hungary

ARTICLE INFO

Article history:
Received 25 February 2019
Received in revised form 23 April 2019
Accepted 17 June 2019
Available online 20 June 2019
Editor: D.F. Geesaman

Keywords:
Inclusive knockout cross sections
Intranuclear cascade model
Eikonal reaction theory

ABSTRACT

Inclusive one- and multi-nucleon removal cross sections have been measured for several Sn, Sb and Te isotopes just beyond the $N = 82$ neutron shell closure. The beams were produced in the projectile fission of a ^{238}U beam at the Radioactive Isotope Beam Factory at RIKEN. The experimental cross sections are compared to predictions from the most recent version of the Liege intranuclear cascade model. Although the overall agreement is good, severe discrepancies are observed for the cases of one- and two-neutron removal from ^{134}Sn and ^{135}Sb projectiles and one-proton knockout from all measured $N = 84$ isotones. These discrepancies, as well as the relevance of quasi-elastic reaction channels to the one-neutron removal cross sections, are discussed. In addition, the measured inclusive one-proton knockout cross section for the semi-magic ^{134}Sn projectile is compared to eikonal direct reaction theory calculations to assess if the suppression factors to these calculated cross sections, deduced from data on reactions of lighter projectile nuclei, are also applicable to heavy nuclei.

© 2019 The Authors. Published by Elsevier B.V. This is an open access article under the CC BY license (http://creativecommons.org/licenses/by/4.0/). Funded by SCOAP[3].

1. Introduction

In the last twenty years, one-nucleon knockout reactions from intermediate energy radioactive ion beams on light target nuclei, such as Be or C, have proved to be a useful tool to study the shell structure of nuclei far from the valley of stability [1,2]. Information concerning active shells at and near the neutron and proton Fermi surfaces in exotic nuclei, and their occupancies, is obtained from a comparison of the experimental inclusive and exclusive one-nucleon knockout cross sections to theoretical direct reaction calculations. To calculate these cross sections, information

* Corresponding author.
E-mail address: andrea.jungclaus@csic.es (A. Jungclaus).

https://doi.org/10.1016/j.physletb.2019.06.035
0370-2693/© 2019 The Authors. Published by Elsevier B.V. This is an open access article under the CC BY license (http://creativecommons.org/licenses/by/4.0/). Funded by SCOAP[3].

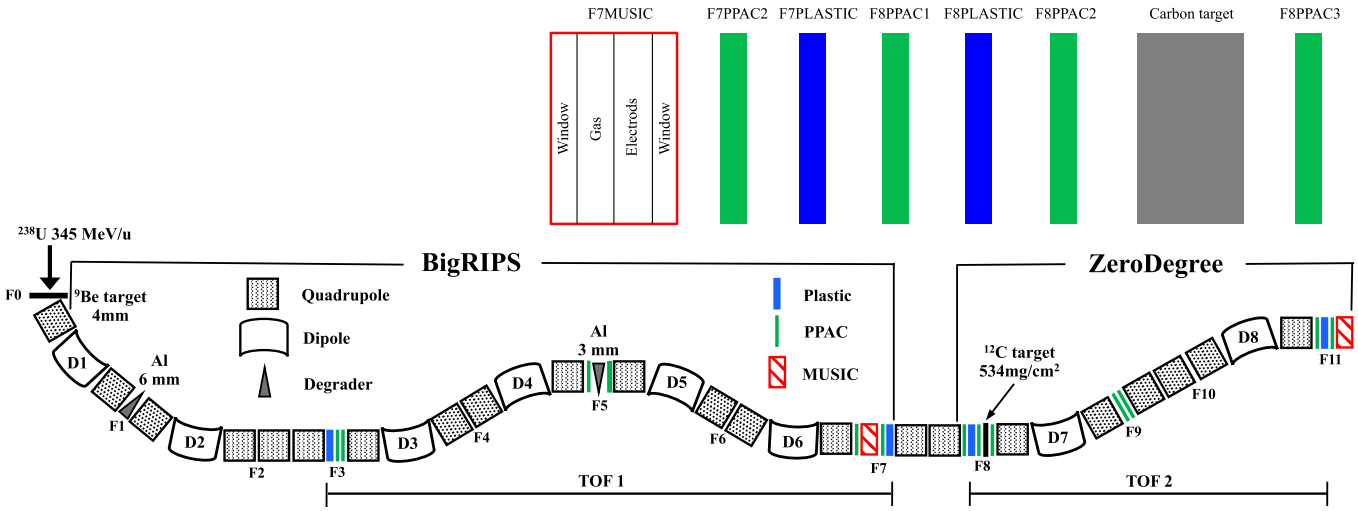

Fig. 1. Schematic view of the BigRIPS and ZeroDegree spectrometers (adopted from Ref. [18]). The material along the beam line between the focal planes F7 and F8, which has been considered in the determination of the correction factor χ in Eq. (2), is shown enlarged in the upper part of the figure.

on the structure of the projectile initial and residual nucleus final states is combined with an approximate description of the reaction dynamics. In most cases this structure information is taken from shell-model calculations employing appropriate model spaces and effective interactions. The reaction dynamics has generally been modeled assuming the sudden (fast collisions) and eikonal (forward scattering) approximations [3,4]. A systematic comparison between the experimental and calculated inclusive (to all bound final states) one-nucleon knockout cross sections, for a large number of light and medium-mass projectile nuclei, evidenced a significant overestimation of the cross section by the calculations [1,2]. The overestimation is more pronounced the larger the binding of the removed nucleon – driven by the neutron-proton asymmetry of the system, $\Delta S = S_n - S_p$ for neutron removal and $\Delta S = S_p - S_n$ for proton removal, with S_p (S_n) the proton (neutron) separation energy. These inclusive cross section systematics have been presented as a suppression factor $R_s = \sigma_{exp}/\sigma_{th}$ as a function of the separation energy asymmetry ΔS [1,2].

While a discrepancy with the model calculations is expected, e.g. due to many-body correlation effects beyond those of truncated-basis shell-model calculations, the magnitude of the observed R_s from the model calculations is not yet understood quantitatively. The observed inclusive cross section systematics have nevertheless been used, see e.g. [5–7], to deduce spectroscopic factors by comparison of the calculations with measured final-state exclusive removal cross sections, taking into account an R_s value consistent with the systematics. In recent years the first one-nucleon knockout experiments have been performed in heavier regions of the nuclear chart [8,9], in particular for nuclei around doubly-magic ^{132}Sn [10–13]. However, before structure information can be deduced from such experiments, it must be clarified whether data and calculations for heavy nuclei conform to the suppression factor, R_s, behavior observed in the lighter mass regions, as collected in Refs. [1,2].

In this Letter, we report on the measurement of one- and multi-nucleon removal cross sections from a number of neutron-rich nuclei beyond the $N = 82$ shell closure, which have been produced with energies around 165 MeV/u at the Radioactive Isotope Beam Facility (RIBF) at RIKEN. The experimental cross sections are compared to the results of calculations performed with the Liege intranuclear cascade model [14–17]. This approach, that describes the nuclear collisions based on a cascade of in-medium, two-body nucleon-nucleon collisions, involves only minimal nuclear structure information – limited to the one-body projectile density. For one-proton knockout from the semi-magic ^{134}Sn projectile, the experimental cross section is also compared to the eikonal model, direct reaction calculations, as discussed above [3,4], in which the projectile structure is taken into account through the single-nucleon overlap functions with the final states of interest and the reaction dynamics are described based on the complex nucleon- and residual nucleus-target optical potentials.

2. Experiment and results

The experiment was carried out at the Radioactive Isotope Beam Factory (RIBF), operated by the RIKEN Nishina Center and the Center for Nuclear Study of the University of Tokyo. A primary beam of ^{238}U at 345 MeV/u bombarded a 4-mm-thick beryllium target located at the entrance of the BigRIPS fragment separator [18] which is sketched in Fig. 1. Fission products around ^{136}Te were selected and purified by employing the Bρ-ΔE-Bρ method through combination of magnetic rigidity (Bρ) selection and two wedge-shaped aluminium degraders. The particle identification was performed on an event-by-event basis using the ΔE-Bρ-TOF method, where the energy loss ΔE was measured by an ionization chamber located at the focal plane F7, Bρ was determined from position measurements using parallel plate avalanche counters (PPACs) and the time of flight (TOF) was measured with two plastic scintillators located at the focal points F3 and F7. The atomic number (Z) and the mass-over-charge (A/Q) ratio of each ion were determined with this method [19]. The resulting particle identification plot is shown in Fig. 2a).

After the selection and identification, the secondary beams were transported to the focal point F8 where they impinged on a 534-mg/cm^2 C target. The energies of the reaction products of interest were in the range 162-170 MeV/u, 138-145 MeV/u and 112-117 MeV before, at the center and behind the target, respectively. Finally, the reaction products as well as the elastically scattered beam ions were identified by the ZeroDegree spectrometer [18] using again the previously described ΔE-Bρ-TOF method. Three slightly different ZeroDegree settings have been used during the experiment. As an example Fig. 2b) shows the ZeroDegree particle identification following the interaction of ^{136}Te ions with the C target from a run in which this nucleus moved on the central trajectories in both BigRIPS and ZeroDegree. As clearly visible in this figure, the ^{136}Te ions, as well as all other reaction products, are

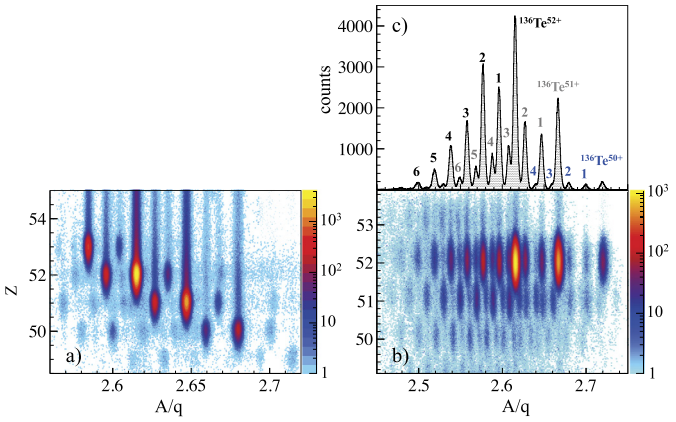

Fig. 2. a) BigRIPS and b) ZeroDegree particle identification plots, the latter for incident ^{136}Te ions detected and identified in BigRIPS. c) Projection of the matrix shown in b) in the range $Z = 51.5$-52.5. The peaks corresponding to the removal of one to six neutrons from the ^{136}Te projectile ions detected in the three different charge states are labelled by numbers.

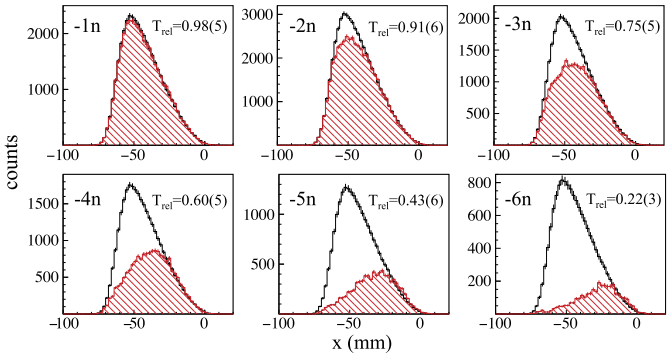

Fig. 3. Distributions of ^{136}Te ions in x direction at the dispersive F5 focal plane for those events in which the isotopes $^{130-135}$Te, populated following the removal of one to six neutrons, were detected in the ZeroDegree spectrometer (red lines) compared to the distribution obtained when unreacted ^{136}Te ions were detected (black lines). In each case, the latter has been downscaled so that both curves coincide on the right wing of the distributions. The resulting values of T_{rel} are quoted for each case.

detected in the ZeroDegree spectrometer in three different charge states, namely fully-stripped, hydrogen-like and helium-like. This results in rather complex A/q distributions as illustrated in Fig. 2c) which shows the A/q distribution for ions with a reconstructed Z in the range $Z = 51.5$-52.5. This figure demonstrates that the A/q resolution of the ZeroDegree spectrometer is sufficient to enable a reliable determination of the number of ions for the reaction products populated following the removal of up to six neutrons.

The cross section for the knockout of a number of neutrons, xn, and protons, yp, from the projectile can be determined from the number of projectile ions impinging on the target, N_{pro}, the number of reaction products in the knockout channel of interest, N_{rp}, and the number of C atoms per cm^2 in the target, n:

$$\sigma_{rp} = \frac{N_{rp}}{n \cdot N_{pro}} \tag{1}$$

with $n = d \cdot N_A / M_{mol}$, calculated from the thickness $d = 534(27)$ mg/cm^2 and the molar mass M_{mol} of the target and the Avogadro constant N_A. Assuming that the losses due to reactions on beam line detectors (plastic detectors, PPACs and MUSICs, see Fig. 1) as well as the efficiency of these detectors is the same for both ion species, the ratio $\frac{N_{rp}}{n \cdot N_{pro}}$ in Eq. (1) can be substituted by the ratio between the respective numbers of ions detected in the ZeroDegree spectrometer, $\frac{N_{rp}^{ZD}}{n \cdot N_{pro}^{ZD}}$, and two correction factors, T_{rel} and χ:

$$\sigma_{rp} = \frac{N_{rp}^{ZD}}{n \cdot N_{pro}^{ZD} \cdot T_{rel}} \cdot \chi \tag{2}$$

T_{rel} is the ratio between the ZeroDegree transmissions for the reaction product and the projectile, $T_{rel} = T_{rp}/T_{pro}$, and the factor χ accounts for the production of the nucleus of interest in reactions on other than the target material. Note that the cross section has to be calculated separately for each charge state (compare Fig. 2) according to Eq. (2) since T_{rel} varies. To determine T_{rel} the spatial distribution of the projectile ions in horizontal direction at the F5 momentum-dispersive focal plane is used. Fig. 3 shows the distributions of ^{136}Te ions separately for those events in which fully stripped $^{130-135}$Te ions, populated via the removal of one to six neutrons from the ^{136}Te projectile, were detected in the ZeroDegree spectrometer. They are compared to the corresponding distribution when fully stripped ^{136}Te ions were detected in the ZeroDegree spectrometer, in each case normalized to the right wing of the distributions which is not cropped by the ZeroDegree acceptance. After this normalization, T_{rel} is then simply obtained as the ratio between the integrals of the two curves. The second correction factor in Eq. (2), χ, takes into account that the nuclei of interest are not only produced in reactions taking place in the C target but also in the detector material along the beam line. More precisely, χ is the ratio between the reactions on the target and the reactions on all material between the ion identification in BigRIPS, i.e. the MUSIC ionization chamber at F7, up to and including the target. As shown in Fig. 1 there are several plastic and PPAC detectors on the beam line in which the reaction of interest can take place. For the present experimental conditions, a value $\chi = 0.83(7)$ has been obtained with the help of LISE++ calculations [20]. The reliability of this approach has been investigated using the data taken with an empty target frame. From this data, an experimental loss factor, $\epsilon_{line} = 0.946(14)$, has been deduced for ^{136}Te which includes both losses due to reactions on beam line detectors and the particle identification efficiency of the ZeroDegree spectrometer. In a second step, the losses due to reactions in the C target, ϵ_{target}, have been determined with the target inserted based on the number of projectile ions detected in BigRIPS and ZeroDegree (separately for each charge state and taking into account the respective ZeroDegree transmission) and ϵ_{line}. The value of $\epsilon_{target} = 0.931(21)$ determined in this way is in perfect agreement with the result of a LISE++ calculation, $\epsilon_{target}^{LISE} = 0.9309$. Further details about the data analysis procedure are provided in Ref. [21].

Following the approach sketched above 0pxn and 1pxn removal cross sections have been determined for all projectiles which have been produced and identified in BigRIPS with sufficient statistics. The results are summarized in Fig. 4 and will be discussed in the following.

3. Discussion

To describe the experimental 0pxn and 1pxn removal cross sections shown in Fig. 4 calculations were performed using two different versions of the Liege intranuclear cascade model (INCL) [14]. This model, which originally had been developed for the description of spallation reactions induced by nucleons, has been extended a few years ago to reactions induced by light ions [15] and in this latter version it can be applied to the experiment discussed here. In this standard version of the model, identical Woods-Saxon type density distributions are used for protons and neutrons. To describe the de-excitation process following the initial cascade stage, the ABLA07 statistical de-excitation model is

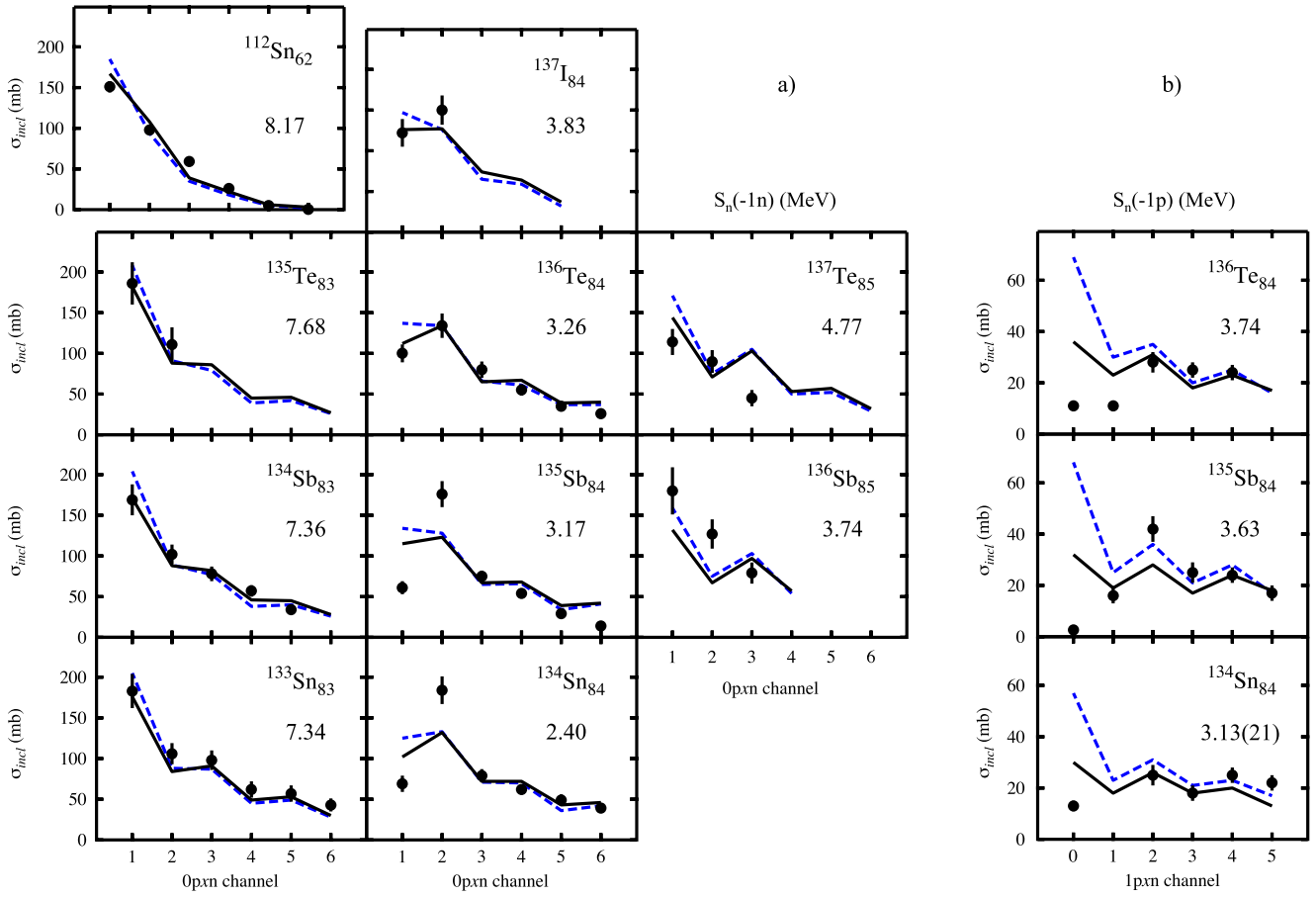

Fig. 4. Comparison between experimental inclusive removal cross sections and the results of calculations performed with the INCL code for a) the 0pxn and b) the 1pxn removal channels. The results obtained following the standard INCL approach [15] are shown as dashed blue lines while the calculations considering realistic proton and neutron densities from HFB calculations and fuzziness parameters f = 0.3 for neutrons and f = 0.5 for protons [17] are shown as solid black lines. In each case the neutron separation energy S_n in MeV [22] of the nucleus populated following a) one-neutron or b) one-proton knockout is quoted. The experimental cross sections for 0pxn removal from ^{112}Sn shown in a) are taken from Ref. [8].

employed [23]. Very recently several refinements have been introduced in the description of the cascade stage of the model aiming for an improvement of the agreement with experiment, in particular for the one-proton knockout channel [16,17]. Two important modifications have been applied: first, more realistic proton and neutron radial density distributions are employed which are obtained either from Hartree-Fock-Bogoliubov (HFB) calculations with a Skyrme interaction [17] or shell model calculations [16]. This refinement may become relevant in the case of heavy neutron-rich nuclei such as the ones studied in the present work. The second modification intents to partially compensate for the neglect of quantum-mechanical effects in the naive INCL picture of the nucleus. A fuzziness parameter is introduced to mimic the fact that in the quantum-mechanical square-well problem, the density outside the well does not vanish, in contrast to the classical INCL picture. The full details and the reasoning behind the applied changes are given in Refs. [16,17]. In the present work, calculations were performed using the HFB densities and standard fuzziness parameters of f = 0.3 for neutrons and f = 0.5 for protons [17]. The results of the calculations using the standard and refined versions of the model are shown as dashed blue and solid black lines, respectively, in Fig. 4. This figure shows an overall good agreement between the calculations and the experimental results. In particular for the 0pxn removal from the $N = 83$ projectiles ^{133}Sn, ^{134}Sb, and ^{135}Te as well as the stable ^{112}Sn [8] (left column in Fig. 4a), i.e. the cases in which nuclear structure effects are washed-out due to the high neutron-separation energy of the 1n daughter nuclei, both the magnitude and the gentle odd-even staggering of the cross sections is nicely reproduced by both calculations. In contrast, none of them correctly describes the measured cross sections for one- and two-neutron removal from the $N = 84$ isotones ^{134}Sn and ^{135}Sb, while for the heavier isotones ^{136}Te and ^{137}I the modifications of the INCL model discussed above clearly improve the agreement with experiment. Taking into account the peculiar structure of nuclei such as ^{134}Sn, with only two valence neutrons above the $N = 82$ shell gap, in combination with the low neutron separation energy, S_n, of the 1n daughter, the failure of the calculations is easily understood [13]. In these cases only the removal of one of the two valence neutrons leads to the population of bound states in the daughter nuclei and thus contributes to the one-neutron removal cross section, while due to the large shell gap the knockout of a neutron from the closed $N = 82$ core populates core-excited states with energies well above the neutron separation energy. These highly-excited states then mainly decay via neutron emission and thus contribute to the measured two-neutron removal cross section. The INCL model, which ignores the shell structure of the nucleus and assumes a continuous energy distribution of the nucleons, is not able to correctly distinguish between knockout from the valence space on the one hand side and removal from the closed core on the other, but reproduces well the sum of the one- and two-neutron removal cross sections as well as the ones for the removal of more than two neutrons. So the conclusion from Fig. 4a) is that for the knockout of neutrons, i.e. the less bound nucleon species in the neutron-rich nuclei

under study, the INCL model describes the experimental results remarkably well as long as nuclear structure effects are negligible. This is even more notable considering that a significant fraction of the total calculated cross section corresponds to the quasi-elastic channel, i.e. events in which the projectile is first excited to high excitation energies followed by the evaporation of one or several nucleons. For example, in the case of the one-neutron knockout reactions studied in the present work, roughly one third of the total cross section corresponds to such two-step processes. Note that these are not considered in the eikonal direct reaction model and therefore, if they indeed turn out to be significant in the region of the nuclear chart discussed in the present work, will need to be taken into account when extracting nuclear structure information from measured one-nucleon knockout cross sections.

Turning now to the one-proton knockout cross sections, Fig. 4b) clearly shows that both calculations fail to reproduce the experimental values for all three studied $N = 84$ projectiles, i.e. ^{134}Sn, ^{135}Sb and ^{136}Te. Note, however, that in this case the refinements, which have been introduced in the modified version of the INCL code, have a much stronger effect as compared to the case of one-neutron knockout, reducing the calculated one-proton knockout cross sections by roughly a factor of two. Already in the past, a similar overestimation of the cross sections for one-proton removal from heavy nuclei by the INCL model has been reported, see for example Refs. [8,16]. In Ref. [24], Glauber model calculations coupled to the ABLA07 code have been performed to describe the one-proton knockout from various Sn projectiles on a C target at higher energies as compared to the present work and also here the calculations yielded far too high cross sections. In that work, this deficiency was cured by an arbitrary increase of the excitation energy of the knockout residue after the cascade stage by 7 MeV. In this way it was possible to adjust the calculated cross sections to experiment. A similar approach, namely an ad hoc increase of the excitation energy before the deexcitation stage, was also followed in the INCL calculations presented in Ref. [25] in order to improve the agreement for a large set of experimental one-proton and one-neutron knockout cross sections. In this case, however, not a constant value as in Ref. [24] but in each case the difference between projectile and daughter separation energies was added to the INCL excitation energy at the end of the cascade stage (for details see Ref. [25]). It is important to notice, however, that any ad hoc increase of the excitation energy of the knockout residue not only leads to the desired decrease of the one-proton knockout cross section, but necessarily implies at the same time an increase of the probability for neutron emission and thus higher cross sections for other reaction channels, in particular 1p1n and 1p2n (one-proton knockout followed by the emission of one or two neutrons), for which unfortunately no experimental results have been reported in Refs. [24,25]. The overall good agreement between calculation and experiment observed in Fig. 4b) for the 1pxn channels with $x > 0$, and in particular the values measured for the 1p1n removal from ^{135}Sb and ^{136}Te, suggest that although seemingly allowing to cure the discrepancy for the one-proton knockout channel, an ad hoc increase of the excitation energy in the INCL calculations is not the right approach to follow in order to uncover the origin of the widely recognized problem the INCL model has in reproducing cross sections for the removal of the more bound nucleon species.

As outlined in the introduction, besides the classical reaction models such as INCL, eikonal direct reaction theory has been used extensively for the calculation of one-nucleon knockout cross sections [3,4]. A basic assumption is that, in the fast, single-nucleon removal from near the surface of a fast-moving projectile with mass A impinging on a light target, the remaining $A-1$ nucleons act as spectators. As a consequence, the probability to find the one-nucleon removal reaction residue in a particular final state reflects the parentage of this configuration in the ground-state wave function of the projectile. The partial cross section for the removal of a nucleon from a single-particle orbital j^π, leading to a given final state α with excitation energy $E^\star_\alpha$ in the mass $A-1$ residue is given by

$$\sigma_{th}(\alpha) = (A/(A-1))^N \cdot C^2S(\alpha, j^\pi) \cdot \sigma_{sp}(j, S^\star_\alpha) \quad (3)$$

where $C^2S(\alpha, j^\pi)$ is the spectroscopic factor and $\sigma_{sp}(j, S^\star_\alpha)$ the single-particle cross section which depends on the effective separation energy $S^\star_\alpha = S_{n,p} + E^\star_\alpha$ [2]. As discussed in the introduction, this model approach has the property that it connects measured knockout cross sections with theoretically-predicted spectroscopic information, namely the spectroscopic factors, $C^2S(\alpha, j^\pi)$. However, to apply the model in the region around ^{132}Sn, it should be clarified if the experimental to theoretical inclusive one-nucleon removal cross section ratio (R_s) systematics of Refs. [1,2] are appropriate also for these heavy nuclear systems.

The theoretical inclusive one-nucleon removal cross section, σ_{th}, is calculated as the sum of the partial cross sections, Eq. (3), to each bound final state of the reaction product. It is assumed that excited final states above the neutron separation energy decay exclusively by particle emission. So, this calculation requires knowledge of the energies and spectroscopic strengths of the final states of the daughter nucleus and has to rely on nuclear structure calculations, performed for example in the frame of the nuclear shell model. For most of the one-nucleon knockout reactions studied in the present work, i.e. one-neutron knockout from $N > 82$ and one-proton knockout from $Z > 50$ nuclei, the calculation of the inclusive cross sections involves large uncertainties due to the unknown excitation energies of the many core-excited states populated in the daughter nuclei. Therefore, unfortunately, in these cases no meaningful conclusion can be drawn from the measured cross sections. The situation is different in the case of one-proton knockout from proton-magic ^{134}Sn projectiles, in which the experimental cross section can be compared to the theoretical model value calculated using Eq. (3). Based on spherical Hartree-Fock and shell model calculations it is assumed that bound states in ^{133}In are populated after knockout from the $1p_{3/2}$, $1p_{1/2}$, and $0g_{9/2}$ orbitals. Shell-model calculations were carried out employing the realistic effective interaction for the $N \geq 82$, $Z \leq 50$ valence space, as were discussed recently in Ref. [26]. For the $1p_{3/2}$ and $1p_{1/2}$ proton-hole single particle energies, relative to the $0g_{9/2}$ orbital, the experimental energies of the $(3/2^-)$ and $(1/2^-)$ states in ^{131}In, namely 1353 and 365 keV [27,28], were employed. Since no ^{133}In excited states information is available from experiment, the removal-reaction calculations use both the shell model excitation energies and spectroscopic factors, listed in Table 1. For all three orbitals listed above, at least 92% of the full strength is carried by

Table 1
Calculation of the inclusive one-proton removal cross section from ^{134}Sn, σ_{th}, based on the excitation energies, E_x, and spectroscopic factors, C^2S, predicted by shell model calculations (see text for details).

I^π	E_x (MeV)	C^2S	σ_{sp} (mb)	$\sigma_{th}(\alpha)$ (mb)
$9/2^+_1$	0.00	9.3	3.26	31.2
$9/2^+_2$	0.81	0.3	3.18	1.0
$1/2^-_1$	0.57	1.9	3.53	6.9
$3/2^-_1$	1.18	1.2	3.46	4.2
$3/2^-_2$	1.62	2.5	3.40	8.7
sum		15.2		52.0

the first two states of each spin, lying below the neutron separation energy of ^{133}In ($S_n = 3.13(21)$ MeV [22]).

A theoretical cross section of $\sigma_{th} = 52.0$ mb is obtained. Regarding the fourth orbital of the $Z = 28$–50 shell, namely $0f_{5/2}$, the single-hole energy of this orbital is experimentally unknown and thus no reliable prediction can be made as to whether knockout will lead to bound states in ^{133}In. We therefore exclude it from the calculation, likewise the small missing strengths from the orbitals considered above, and thus take the calculated theoretical cross section as a lower limit, $\sigma_{th} > 52.0$ mb. From this and the experimental value, $\sigma_{exp} = 13(2)$ mb, we determine an approximate upper limit on the suppression factor, $R_s = \sigma_{exp}/\sigma_{th} < 0.25(4)$. The associated separation energy asymmetry, ΔS, calculated from the cross-section weighted average of the $S^{\star}_{\alpha}$ values to the bound final states is $\Delta S = 13.1$ MeV. Comparison with the light nucleus R_s systematics [1,2], using the approximate parametrization of Ref. [6], one would expect an $R_s^{sys} \approx 0.4$ for such a value of ΔS. In the range $\Delta S = 12$-14 MeV, four R_s values have been derived, the two most accurate for one-proton knockout being for ^{10}Be ($R_s = 0.42(2)$ [29]) and ^{36}Si ($R_s = 0.39(2)$ [5]). These values significantly exceed the limit suggested from the present analysis.

We note that, if one employs a single-hole energy for the $0f_{5/2}$ orbital (relative to $0g_{9/2}$) of 2.6 MeV, as has been used in the literature [27,30–33], then the shell model calculation used here attributes a spectroscopic factor of 4.7 to the sixth $5/2^-$ state at an excitation energy of 2.68 MeV, below S_n, so that R_s would be further reduced. Spherical Skyrme Hartree-Fock calculations, on the other hand, using the SkX and Sly4 interactions, place this $0f_{5/2}$ hole energy at 4-5 MeV [34,35]. An energy of 3.8 MeV is expected on the basis of the nuclear monopole Hamiltonian which was adjusted to a large number of experimental energies of particle and hole states outside double magic cores all over the chart of nuclides by Duflo and Zuker [36]. Furthermore, the R_s analysis presented above relies on high purities of the proton-hole states in ^{131}In (similar to the ones measured for neutron-hole and neutron-particle states in ^{131}Sn and ^{133}Sn, respectively [37,38]) and that the shell-model calculations provide a realistic treatment of the effects of nucleon-nucleon correlations upon the valence orbitals. Clearly, more exclusive experimental information is required to validate these assumptions in order that one-nucleon removal reactions might be used to extract spectroscopic information in the region around ^{132}Sn. As such data become available for nuclei south-east of ^{132}Sn, then alternative shell-model approaches using extended valence spaces, see e.g. Refs. [39–41], can be used to assess the systematic uncertainties inherent in the nuclear structure model description presented here.

4. Summary

We reported on the measurement of inclusive one- and multi-nucleon removal cross sections for several Sn, Sb and Te isotopes just beyond the $N = 82$ neutron shell closure. The experimental results were compared to INCL model calculations. In general, good agreement was found for the removal of one or several neutrons, i.e. the less bound nucleon species in these region of the nuclear chart. The only exceptions are the cases of one- and two-neutron removal from ^{134}Sn and ^{135}Sb, which are dominated by strong nuclear structure effects. A detailed analysis of the INCL calculations showed that, in all cases studied, roughly one third of the one-neutron knockout cross section corresponds to quasi-elastic processes. For one-proton knockout on the other hand, the INCL model clearly overestimates the inclusive cross section, a trend which has already been reported in the literature. The present data for multi-nucleon removal indicate that an ad-hoc increase of the excitation energy in the INCL model at the end of the cascade process, an approach which has been suggested to cure the incapacity of the model to correctly describe the removal of deeply bound nucleons, does not address the origin of this problem. Finally, the experimental inclusive cross section for one-proton removal from semi-magic ^{134}Sn was compared with calculations based on eikonal direct reaction theory with structure information from the nuclear shell model. The limit this places on the derived suppression factor, R_s, is lower than from the systematics derived from similar analyses of inclusive cross section data for lighter nuclei, and alerts that more experimental information is needed before such one-nucleon removal reaction systematics should be used to deduce spectroscopic information in the region of heavy nuclei around ^{132}Sn.

Acknowledgements

We thank the staff of the RIKEN Nishina Center accelerator complex for providing high-intensity beams to the experiment. This work was supported by the Spanish Ministerio de Economía y Competitividad under contracts FPA2014-57196-C5-4-P and FPA2017-84756-C4-2-P. J.A.T. acknowledges the support of the Science and Technology Facilities Council (UK) grant ST/L005314/1 and R.O. that of JSPS KAKENHI Grant No. 26887048. G.M.T. gratefully acknowledges funding of this research from the Research Council of Norway, Project Grant No. 222287.

References

[1] A. Gade, et al., Phys. Rev. C 77 (2008) 044306.
[2] J.A. Tostevin, A. Gade, et al., Phys. Rev. C 90 (2014) 057602.
[3] J.A. Tostevin, Nucl. Phys. A 682 (2001) 320.
[4] P.G. Hansen, J.A. Tostevin, Annu. Rev. Nucl. Part. Sci. 53 (2003) 219.
[5] S.R. Stroberg, et al., Phys. Rev. C 90 (2014) 034301.
[6] A. Mutschler, et al., Phys. Rev. C 93 (2016) 034333.
[7] H.L. Crawford, et al., Phys. Rev. C 95 (2017) 064317.
[8] L. Audirac, et al., Phys. Rev. C 88 (2013) 041602(R).
[9] G. Cerizza, et al., Phys. Rev. C 93 (2016) 021601(R).
[10] H. Wang, et al., Phys. Rev. C 88 (2013) 054318.
[11] H. Wang, et al., Prog. Theor. Exp. Phys. 2014 (2014) 023D02.
[12] H. Wang, et al., Phys. Rev. C 94 (2016) 051301(R).
[13] V. Vaquero, et al., Phys. Rev. Lett. 118 (2017) 202502.
[14] A. Boudard, et al., Phys. Rev. C 87 (2013) 014606.
[15] D. Mancusi, et al., Phys. Rev. C 90 (2014) 054602.
[16] D. Mancusi, et al., Phys. Rev. C 91 (2015) 034602.
[17] J.L. Rodríguez-Sánchez, et al., Phys. Rev. C 96 (2017) 054602.
[18] T. Kubo, et al., Prog. Theor. Exp. Phys. 2012 (2012) 03C003.
[19] N. Fukuda, T. Kubo, T. Ohnishi, N. Inabe, H. Takeda, D. Kameda, H. Suzuki, Nucl. Instrum. Methods B 317 (2013) 323.
[20] D. Bazin, et al., Nucl. Instrum. Methods A 482 (2002) 307.
[21] Victor Vaquero Soto, PhD thesis, Universidad Autónoma de Madrid, 2018.
[22] M. Wang, et al., Chin. Phys. C 36 (2012) 1603.
[23] A. Kelic, M.V. Ricciardi, K.-H. Schmidt, Joint ICTP-IAEA Advanced Workshop on Model Codes for Spallation Reactions, Report INDC(NDC)-0530, IAEA, Trieste, Italy, 2008, p. 181.
[24] J.L. Rodríguez-Sánchez, et al., Phys. Rev. C 96 (2017) 034303.
[25] N. Paul, et al., Phys. Rev. Lett. 122 (2019) 162503.
[26] A. Jungclaus, et al., Phys. Rev. C 93 (2016) 041301(R).
[27] J. Taprogge, et al., Phys. Rev. Lett. 112 (2014) 132501.
[28] A. Kankainen, et al., Phys. Rev. C 87 (2013) 024307.
[29] G.F. Grinyer, et al., Phys. Rev. C 86 (2012) 024315.
[30] J. Taprogge, et al., Phys. Lett. B 738 (2014) 223.
[31] J. Taprogge, et al., Phys. Rev. C 91 (2015) 054324.
[32] A. Jungclaus, et al., Phys. Rev. C 94 (2016) 024303.
[33] A. Jungclaus, et al., Phys. Lett. B 772 (2017) 483.
[34] E. Chabanat, P. Bonche, P. Haensel, J. Meyer, R. Schaeffer, Nucl. Phys. A 635 (1998) 231.
[35] B.A. Brown, Phys. Rev. C 58 (1998) 220.
[36] J. Duflo, A.P. Zuker, Phys. Rev. C 59 (1999) 2347(R).
[37] K.L. Jones, et al., Nature 465 (2010) 454.
[38] R. Orlandi, et al., Phys. Lett. B 785 (2018) 615.
[39] H. Naidja, F. Nowacki, K. Sieja, Acta Phys. Pol. B 46 (2015) 669.
[40] C. Yuan, et al., Phys. Lett. B 762 (2016) 237.
[41] T. Togashi, et al., Phys. Rev. Lett. 121 (2018) 062501.